Chemistry–A European Journal
Research Article
doi.org/10.1002/chem.202201297
Chemistry Europe
European Chemical Societies Publishing

www.chemeurj.org

Optical Modulation of Antibiotic Resistance by Photoswitchable Cystobactamids

Giambattista Testolin[+],[a] Jana Richter[+],[a] Antje Ritter,[a] Hans Prochnow,[a] Jesko Köhnke,[b] and Mark Brönstrup*[a, c, d]

Abstract: The rise of antibiotic resistance causes a serious health care problem, and its counterfeit demands novel, innovative concepts. The combination of photopharmacology, enabling a light-controlled reversible modulation of drug activity, with antibiotic drug design has led to first photoswitchable antibiotic compounds derived from established scaffolds. In this study, we converted cystobactamids, gyrase-inhibiting natural products with an oligoaryl scaffold and highly potent antibacterial activities, into photoswitchable agents by inserting azobenzene in the *N*-terminal part and/or an acylhydrazone moiety near the *C*-terminus, yielding twenty analogs that contain mono- as well as double-switches. Antibiotic and gyrase inhibition properties could be modulated 3.4-fold and 5-fold by light, respectively. Notably, the sensitivity of photoswitchable cystobactamids towards two known resistance factors, the peptidase AlbD and the scavenger protein AlbA, was light-dependent. While irradiation of an analog with an *N*-terminal azobenzene with 365 nm light led to less degradation by AlbD, the AlbA-mediated inactivation was induced. This provides a proof-of-principle that resistance towards photoswitchable antibiotics can be optically controlled.

Introduction

The last decade witnessed the rise of photopharmacology, a research area that relies on the concept that stable isomeric forms of a molecule can be interconverted to each other by light of different wavelengths in a reversible and repetitive manner.[1] Because the isomers differ by their three-dimensional shape, their interactions with biological targets and the resulting pharmacological effects are light-controllable by 'photoswitching'. The successful conversion of a bioactive compound to a photoresponsive agent requires the identification of an appropriate site on the scaffold where a photoswitchable group can be inserted. Azobenzene and its analogs have been by far the most widely applied photoswitches, but also other types such as diarylethene, spiropyran, acylhydrazone, iminothioindoxyl have been developed and functionally validated.[2]

Antimicrobial resistance renders currently used antibiotics continuously less efficacious. In consequence, infections by pathogenic bacteria have become again a serious threat to public health.[3] Fighting resistance increasingly follows a 'One Health' strategy, taking into consideration that resistance spreads not only among humans (e.g. in hospitals), but also in the environment and in animal livestock.[4] The discovery of new antibiotics is therefore of high importance for human health, and also unconventional strategies to control and slow down resistance development are highly desirable.[5] Among those, photoresponsive antibiotics have been proposed, because they offer the advantage of a body site selective control of activity, thus limiting off-target effects on commensal microbiota.[6] In addition, they have the potential to limit the development of bacterial resistance, if they reside in an inactive state without exerting selection pressure once secreted to the environment. First examples on photoswitchable antibiotics based on quinolones, gramicidin/tyrocidine, or trimethoprim have been realized.[2g,6–7] Recently, Lauxen et al. have studied bacterial resistance mechanisms of trimethoprim photoswitchable conjugates, but differences between *cis* and *trans* isomers were subtle.[8]

This study reports the introduction of photoswitches into a new class of antibiotics that is not used clinically yet. Cystobactamids like 861-2 (**1**) and the structurally related albicidin (**4**) are microbial natural products with novel and

[a] *Dr. G. Testolin,[+] Dr. J. Richter,[+] A. Ritter, Dr. H. Prochnow, Prof. Dr. M. Brönstrup*
Department of Chemical Biology
Helmholtz Centre for Infection Research
Inhoffenstrasse 7 38124 Braunschweig (Germany)
E-mail: mark.broenstrup@helmholtz-hzi.de
Homepage: https://www.helmholtz-hzi.de/broenstrup

[b] *Prof. Dr. J. Köhnke*
Helmholtz Institute for Pharmaceutical Research Saarland (HIPS)
Saarland University, Campus E8.1, 66123 Saarbrücken (Germany)

[c] *Prof. Dr. M. Brönstrup*
German Center for Infection Research (DZIF)
Site Hannover-Braunschweig, 38124 Braunschweig (Germany)

[d] *Prof. Dr. M. Brönstrup*
Center of Biomolecular Drug Research (BMWZ)
Leibniz University
30159 Hannover (Germany)

[+] *These authors contributed equally to this work.*

Supporting information for this article is available on the WWW under https://doi.org/10.1002/chem.202201297

unique structural features (Figure 1) and have high activity against a broad range of Gram-negative and -positive pathogens by targeting bacterial gyrase.[9] Two resistance factors for albicidin have been well characterized,[10] the endopeptidase AlbD that cleaves albicidin into two inactive fragments, and the high affinity binder AlbA that traps the natural product and thereby neutralizes its antimicrobial activity. Cystobactamids are also substrates for AlbD,[11] while how far their antibiotic function is hampered by AlbA is still unclear.

Total synthesis and medicinal chemistry efforts by us and others[12] led to an understanding of structure-activity relationships and also to the first analog CNDM-861 (**2**) that showed high efficacy in vivo in a mouse infection model.[11] Based on this knowledge, we aimed at preparing photoresponsive analogs, and report the design, synthesis and characterization of mono- and double-photoswitchable cystobactamids in this communication. In addition to exploring differences in antimicrobial properties between the isomeric states, we also report a proof of principle that bacterial resistance can be modulated with light and propose an alternative concept for the application of photoswitchable antibiotics.

Results

N-terminally modified cystobactamids

The oligopeptidic, aromatic nature of the cystobactamids makes them an ideal substrate for *azologization*.[13] Previous SAR studies have shown that the amide bond connecting rings A and B can be replaced by other functional groups without loss of activity. We therefore decided to replace the *N*-terminal dipeptide with azobenzenes. A set of three azobactamids was synthesized that differed by their *para*-substituents on the A-ring, enriching the electronic density (as in **6b**) or decreasing it (as in **6c**) compared to the unsubstituted **6a** (Figure 2A). In **6d**, the amide bond was replaced by an acylhydrazone moiety, which has not been used in photopharmacology so far. The variable part of the molecules was introduced in the last step of the synthesis by coupling the Eastern tetrapeptidic portion of the scaffold, whose synthesis has been previously reported,[11] with the photoswitchable unit (see the Supporting Information, page 29).

To assess its photo-properties, a 0.5 mM DMSO solution of azobactamid **6a** was exposed to 365 nm light at time interval of 10 min to induce a *trans*→*cis* isomerization, and to 450 nm light to reverse the *cis*-isomer back to the *trans* state (Figure 2B). The UV spectrum after irradiation displayed an additional shoulder at 260 nm, had a weaker maximal absorption at 314 nm, and an additional maximum at 428 nm (Figure 2C). Quantification of the two isomers was carried out by liquid chromatography coupled to UV detection and mass spectroscopy (LC/UV/MS). *Cis*- and *trans*-isomers had baseline-separated retention times of 13.8 and 15.0 minutes, respectively, and a fraction of 52% of the *cis*-form could be obtained in the photostationary state (PSS) (Figure 2D). We noted that the *cis*/*trans* ratio at the PSS was concentration and solvent dependent[14] and varied from 0.8 at 0.1 mM to 0.35 at 1 mM in DMSO (Supporting Information Figure S7).

Thermal relaxation from the PSS to the ground state occurred with a half-life of 13.8 h at 35 °C, a value that is compatible for biological applications. By determining the reaction rates (k) for the thermal relaxation at different temperatures, an activation energy (E_A) of 118.95 kJ/mol was calculated for **6a**.

Next, the antimicrobial properties were assessed by determining the minimal inhibitory concentration (MIC) of compounds needed for inhibiting the growth of the Gram-negative bacterium *Escherichia coli* BW25113 (Table 1). The solutions of antibiotics (0.5 mM in DMSO) were either kept in the dark or irradiated with light of 365 nm, and then added to the bacterial culture, followed by a 18 h incubation period. Azobactamids **6a**–**6c** showed excellent antimicrobial potencies in the sub-μg/mL range, while hydrazobactamid **6d** possessed diminished activity, thus indicating that an azo group represents a better bioisosteric substitution for the amide connecting rings A and B

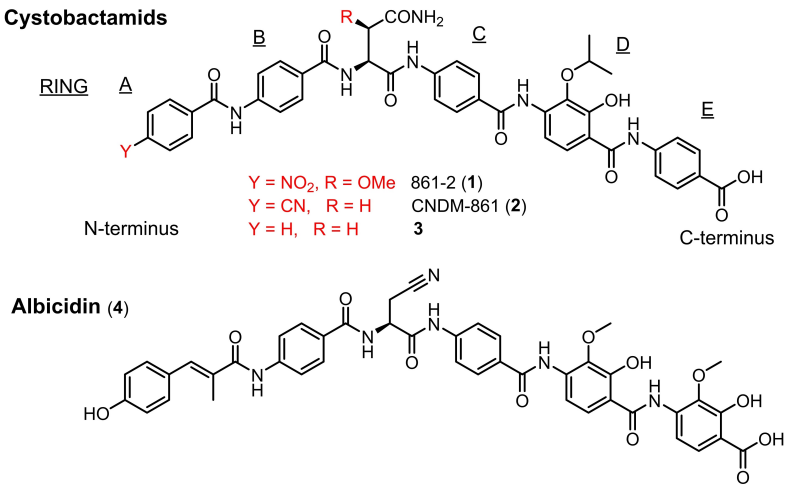

Figure 1. Chemical structures of natural and synthetic cystobactamids and of albicidin.

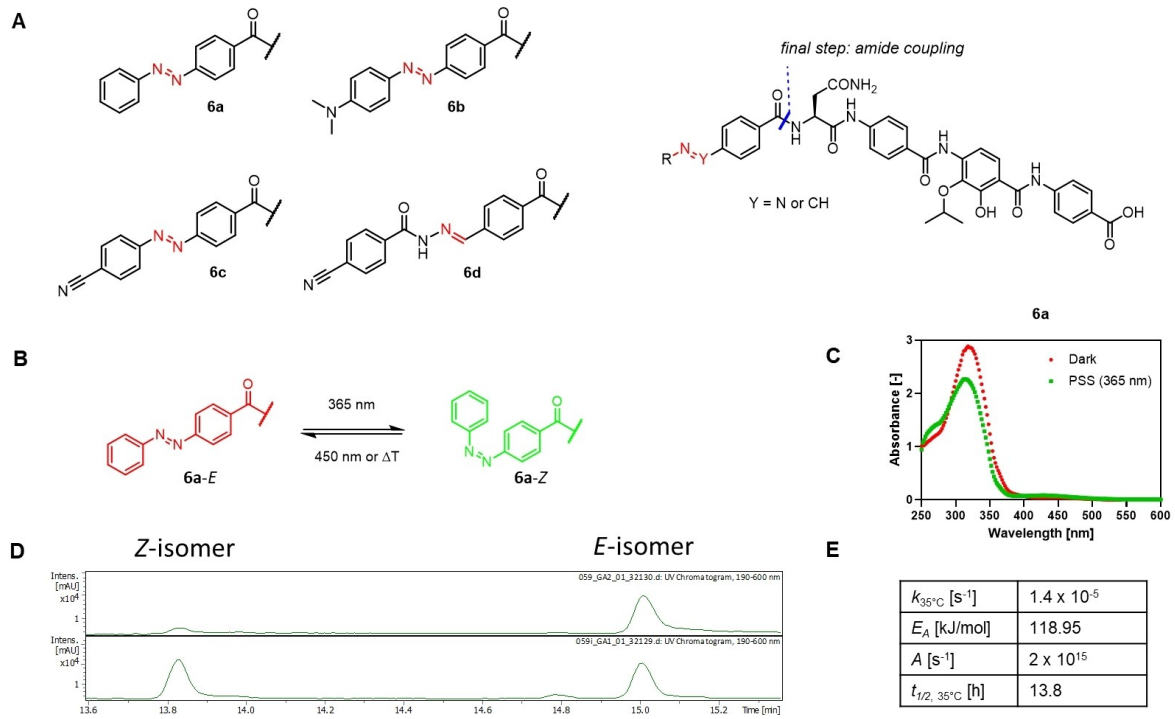

Figure 2. Cystobactamids with *N*-terminal photoswitches. A) Compound structures. Photoswitchable functional groups are highlighted in red, and the final synthetic step connecting the shown *N*-terminal A–B rings to the Eastern part is indicated in blue; B) E→Z isomerization of **6a**; C–E) Characterization of **6a**; C) UV spectra of **6a** (0.5 mM in DMSO) before irradiation (in red) and after irradiation with 365 nm light (in green); D) LC/UV-chromatographic traces before irradiation (above) and after irradiation with 365 nm light (below); E) calculated kinetic parameters: rate constant *k*, activation energy E_A, preexponential factor *A*, half-life $t_{1/2}$.

Table 1. Antimicrobial and enzymatic activities of selected cystobactamids with a single photoswitch.[a]

Compound	MIC [μg/ml]		Gyrase IC_{50} [μM]	
	Dark	365 nm	Dark	365 nm
2	0.005	–	0.08	–
6a	0.35	0.18 (1.9)	1.4	1.1 (1.3)
6c	0.64	0.45 (1.4)	0.5	0.1 (5.0)
6d	4.37	1.54 (2.8)	nd	nd
10a	0.01	0.01 (1)	1.1	1.0 (1.1)
10f	0.04	0.1 (0.4)	nd	nd
10j	0.10	0.34 (0.3)	nd	nd

[a] Thermally adapted state (dark) compared to the PSS following 365 nm irradiation. The MIC was determined on *E. coli* BW25113 by fitting a Gompertz equation to the growth inhibition curve, and the enzymatic activity was determined with an *E. coli* gyrase supercoiling assay. Numbers in brackets display the fold-difference in activity between dark vs. irradiated states. nd = not determined.

than an acylhydrazone. For all compounds, the irradiated samples showed enhanced, up to 2.8 fold improved antimicrobial properties.

Compound **6b** possessed a potent MIC of 0.13 μg/ml, but as could be expected due to the *para*-amino moiety on the azobenzene,[2a] its half-life was too short to retain photoisomerization on a time scale useful to asses antimicrobial properties (Supporting Information Figure S1).

We wondered whether the difference in activity was due to changes in affinity for the enzymatic target or to permeation properties into the bacterial cells. To address this, azobactamids were tested in vitro in a gyrase negative supercoiling assay. The relative activities observed in the cell-based assay were reflected in vitro: Irradiated samples showed up to five-fold higher gyrase inhibition compared to the thermally adapted ones.

C-terminally modified hydrazobactamids

We hypothesized that configurational changes at the *C*-terminus of the molecule may have an even higher impact on activity. This was justified by the fact that ring D is an essential pharmacophore of the cystobactamids, featured by a phenol group that is particularly acidic due to an interaction with the amide connecting rings D and E.[15] We thus decided to replace the amide bond, but considered that acylhydrazones were a more suitable moiety than azobenzenes to retain the electronic properties of the original amide, at the same time offering *trans-cis* photoisomerization of the C–N double bond. The E ring was chosen as either a substituted phenyl or a heterocycle possessing different properties (acidic, neutral or weakly basic) (Scheme 1). In **10b**, **d**, and **e**, fluorine or chlorine atoms were introduced at the *ortho*-positions following the same principle applied to azobenzenes, in order to generate red-shifted acylhydrazones with isomeric states possessing separated n→π* absorption bands.[16] The pyrazoles **10g–j** were inspired

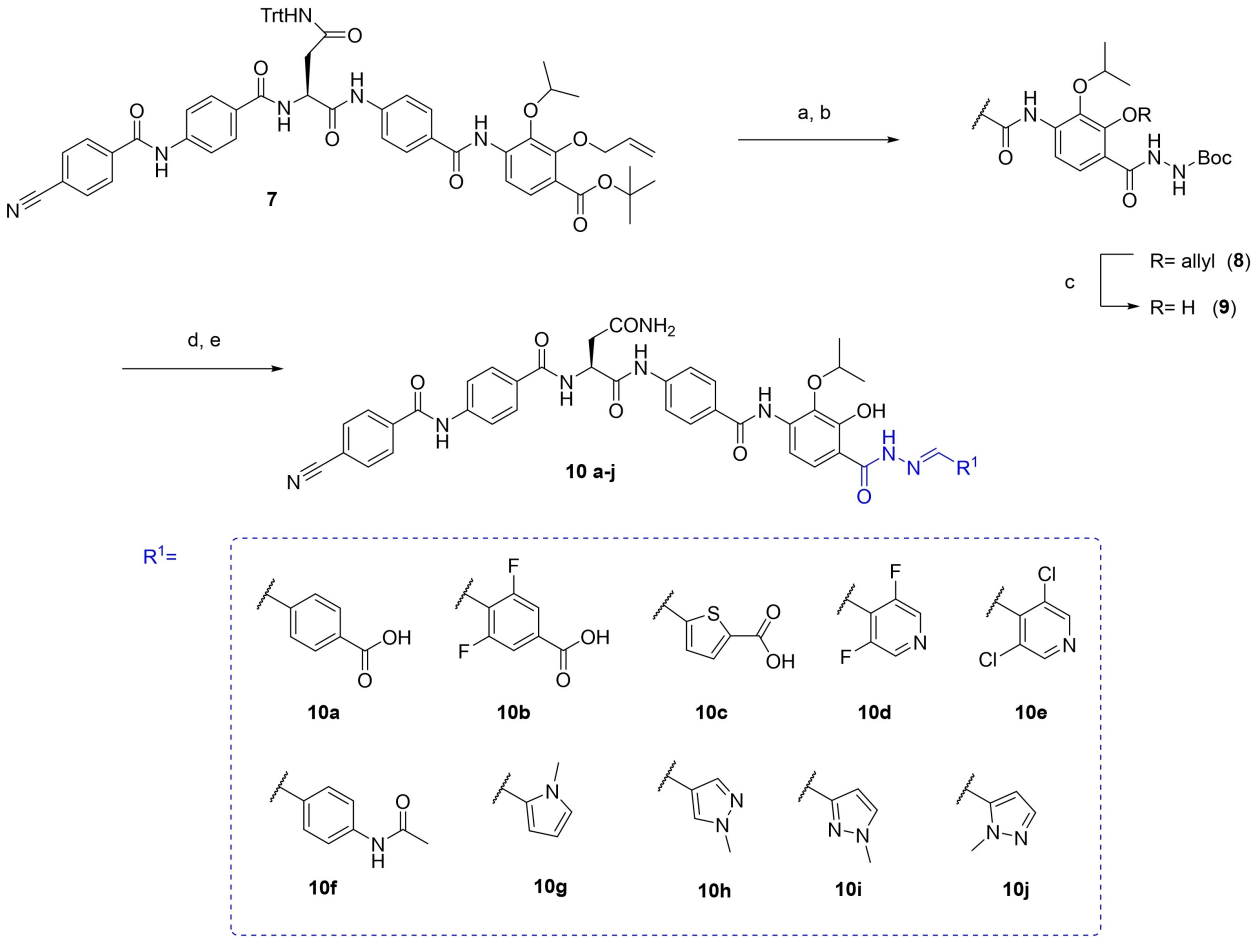

Scheme 1. Final steps for the synthesis of C-terminal hydrazobactamids and overview of synthesized analogs. Reagents, conditions, isolated yields: a) DCM, TFA, TiPS, rt, 2.5 h, quant.; b) HATU, DiPEA, DMF, rt, 15 min, then tert-butyl carbazate, rt, 3 h, 91%; c) Pd(PPh3)4, PhSiH3, THF rt, 2.5 h, 60%; d) DCM, TFA, rt, 2 h, quant.; e) aldehyde in THF, rt, 15 min, 10–81%.

by the azoheteroarene photoswitches reported by Weston et al., who observed quantitative E→Z isomerization and very long half-lifes.[17] For the synthesis of all analogs, we relied on the robust chemistry of acylhydrazone condensation, and employed it as the last synthetic step to enable an efficient late stage diversification. Ten *C*-terminally modified hydrazobactamids were synthesized in five steps from known pentapeptide intermediate **7**.[11]

A characterization of the photoinduced isomerization by LC/UV/MS was not possible, because irradiated and non-irradiated compounds had identical retention times. However, the UV spectra of the compounds were clearly different pre- and post-irradiation (Figure 3B and Supporting Information Figure S2). For instance, the absorbance spectrum of **10c** showed a shoulder above 400 nm in the thermally adapted state, which rose to two distinct maxima at 408 and 430 nm after irradiation. On the other hand, a maximum at 354 nm had a strongly decreased intensity. The photoisomerization could be reverted by irradiation with light of 450 nm, and the compound showed a limited degree of fatigue (on average 3.5% per cycle, Figure 3C). This has been reported for other thiophene-derived acylhydrazones and attributed to structural rigidity and its effects on thiophene C–C vibrations.[18] The λ_{max} of the PSS at 430 nm is shifted by 10–30 nm to the visible range compared to related, known thiophenyl hydrazones, which might be due to the presence of the carboxylic acid. The introduction of fluorine in **10b** did not induce the expected shift of the n→π* absorption band, but led to a higher maximum compared to **10a** (Supporting Information Figure S6).

The antimicrobial properties were assessed by MIC determinations against *E. coli* for thermally adapted and irradiated samples as described above. For **10d, f, i** and **j** the thermally adapted forms were up to 3.4-fold more potent, while all other compounds remained equipotent (Table 1 and Supporting Information Table S1). Thus, we obtained a trend that was opposite to the one obtained for single photoswitches. The hydrazobactamids **10a** and **10c** were the most potent compounds of this study with MIC's as low as 10 and 30 ng/ml for both forms, respectively (Table 1 and Supporting Information Table S1). The introduction of fluorine atoms at the *ortho*-position (**10b**) or the replacement of the *para*-aminobenzoic acid unit by heterocycles was tolerated but lowered the antimicrobial potency.

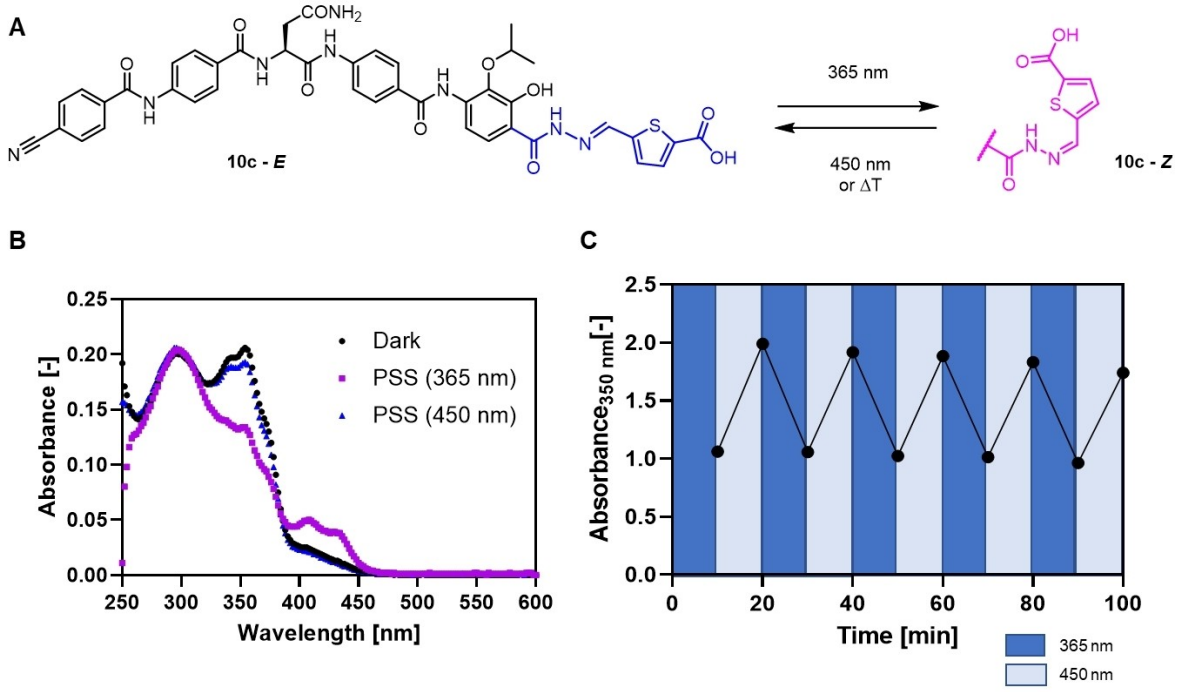

Figure 3. Characterization of hydrazobactamid **10c**. A) Chemical structure and photo-inducible E→Z isomerization of acylhydrazone moiety (highlighted in blue and violet); B) UV spectra of **10c** (0.5 mM in DMSO) in its thermally adapted state before irradiation (in black) and after irradiation with 365 nm light (in violet) and with 450 nm light (in blue); C) Photoswitching cycles, recorded by the UV absorption at 350 nm after alternating irradiation with 365 nm light (light blue periods) and 450 nm (dark blue periods).

Doubly photoswitchable cystobactamids

To investigate whether differences in antimicrobial potency were additive or not, we considered the simultaneous incorporation of both *N*- and *C*-terminal structural variations, giving rise to unprecedented doubly photoswitchable compounds. Initially, the *N*- and *C*- terminal residues for which irradiated samples gave the same activity trend were combined to achieve additive effects. To this end, the plain azobenzene of **6a** was combined with acidic acylhydrazones. Furthermore, in order to obtain molecules that can be selectively isomerized only at the *N*-terminus, a red-shifted, tetrahalogenated azobenzene was coupled with selected acylhydrazones (Scheme 2B). Such compounds may allow to exploit the concept of orthogonal control of photoswitching properties, that has been demonstrated with structurally different photoswitches before.[19] Ideally, such molecules would enable multiple controls of activity by selective *N*-terminal isomerization upon exposure to green light, and double photoswitching by irradiation with 365 nm light.

Retrosynthetically, the formation of the acylhydrazone was envisioned as the final synthetic step, preceded by the introduction of the *N*-terminal photoswitchable moiety. The known tripeptide **15** represented a key intermediate for the synthesis of the target compounds (Scheme 2B). Initially, the primary amino group was transformed into the corresponding trifluoroacetamide (66%) to enable derivatization of the *C*-terminal carboxylate. The orthogonally protected tripeptide was then treated with trifluoroacetic acid to deprotect the Trt-modified amide and the *C*-terminal carboxylate at the same time; the latter was converted into an *N*-Boc protected acylhydrazine that was directly subjected to aminolysis of the trifluoroacetamide using ammonia in methanol to liberate the primary, aliphatic amine, obtained with a 48% yield over the three steps. Amine **16** was then linked to the azobenzene moieties (**14a–c**) using HATU as a coupling reagent that cleanly afforded the corresponding O-allyl-N-Boc-tetra peptides, that underwent palladium-catalyzed de-allylation of the phenol on ring D using phenyl silane as a nucleophilic scavenger to obtain **18a–c**. Partial concomitant reduction of the azo moiety was observed for **18a** and **18c** that decreased the yield over the two steps (20-60%). The final steps of the synthesis consisted of an acidic N-Boc deprotection, followed by condensation with the aldehyde of interest and final purification of the target molecule by preparative reversed-phase (RP)-HPLC under basic conditions (19–58%).

The tetrahalogenated azobenzenes carrying a carboxylate were obtained by a nucleophilic attack of an aryl lithium species to an aryl diazonium salt, similar to the route reported by Feringa and coworkers (Scheme 2A).[20] The use of lithium tetramethylpiperidine (LTMP) as the lithiating reagent instead of butyl lithium enabled broader functional group tolerance in the presence of both ester and nitrile functions on the reaction substrates.

Three sets of doubly photoswitchable cystobactamids were synthesized, comprising six compounds overall (**19a**, **19b**, **20a, 20b**, **21b, 21c**, Scheme 2B). An assessment of the antimicrobial

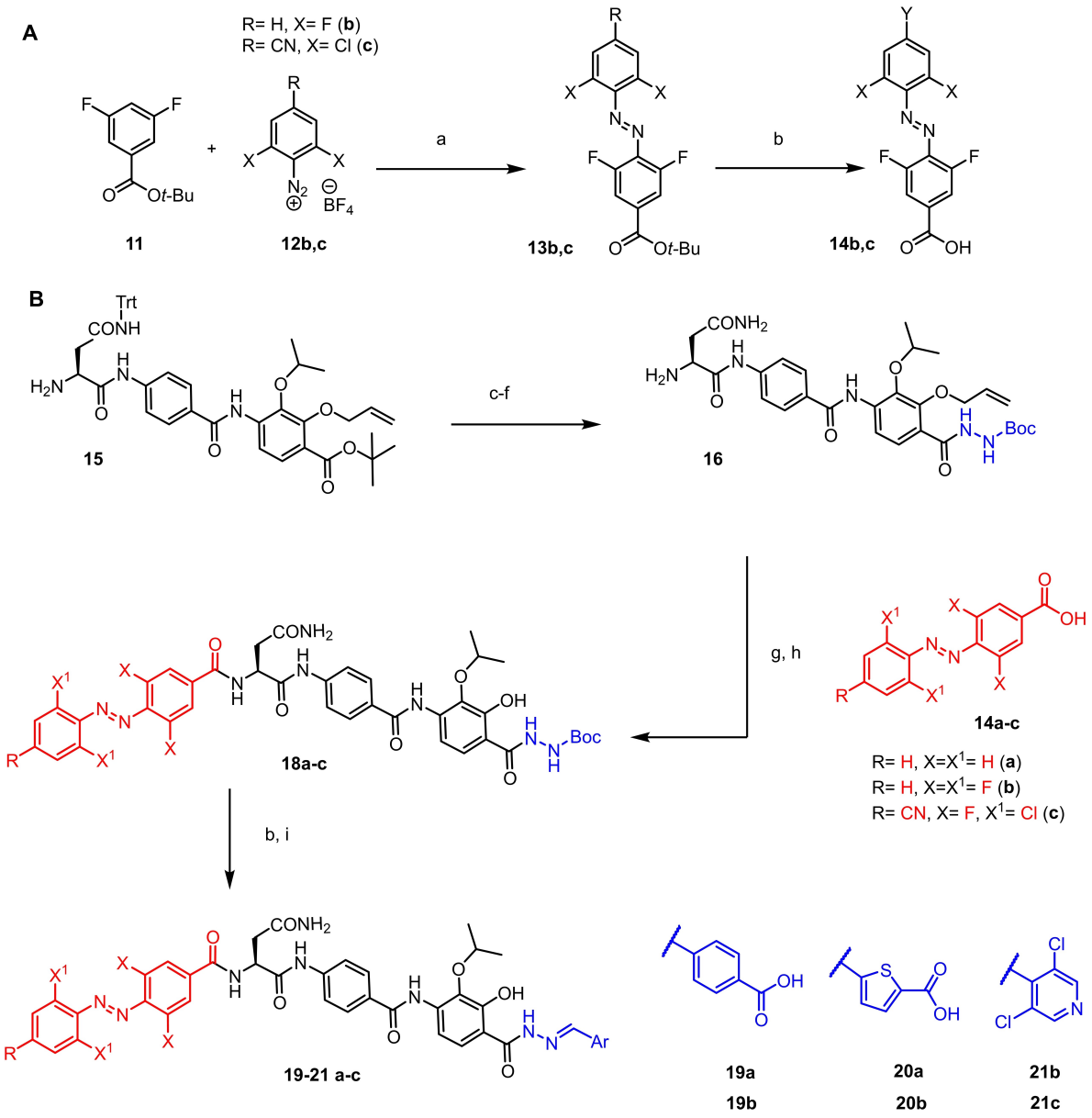

Scheme 2. A) Synthesis of red-shifted azobenzenes; B) Synthetic route to doubly photoswitchable cystobactamids. Photoswitchable moieties are highlighted in blue and red. Reagents, conditions, isolated yields: a) LTMP, THF, −78 °C 30 min, then **12** in THF −85 °C, 2 h, 49–51 %; b) DCM, TFA, rt, 2 h; quant; c) TFAA, TEA, DCM, rt, 4 h, 66 %; d) DCM, TFA, TiPS, rt, 2.5 h; e) HATU, DiPEA, DMF, rt, 30 min then tert-butyl carbazate, rt, 3 h; f) NH_3 (7 N) in MeOH, THF, 45 °C, 10 *h*, 48 % 3 steps; g) **14a–c**, HATU, DiPEA, DMF, rt, 30 min then **16** rt, 1 h; h) $Pd(PPh_3)_4$, $PhSiH_3$, THF rt, 2.5 h, 20–60 % 2 steps; i) aldehyde in THF, rt, 15 min., 19–58 %.

properties revealed that four of the compounds were not inhibiting growth of *E. coli* up to 6.4 μg/mL, the highest concentration tested (Table 2 and Supporting Information Table S1). Only **19a** and **20a**, bearing unsubstituted A and B rings, showed MICs in a therapeutically useful window, while the introduction of halogens in the *ortho*-position was not tolerated. The biological inactivity was paralleled by a loss of gyrase inhibitory capacity. We therefore focused on **19a** and **20a** that had plain azobenzene at the *N*-terminus and either benzoate or thiophene carboxylic acid at the *C*-terminus.

A selective photoisomerization control of **19a** and **20a** was not possible due to the overlapping absorption spectra of the

Table 2. Antimicrobial and enzymatic activities of selected doubly photoswitchable cystobactamids.[a]

Compound	MIC [μg/ml]			Gyrase IC_{50} [μM]	
	Dark	365 nm	450 nm	Dark	365 nm
19a	0.40	0.28 (1.4)	1.12 (0.4)	1.0	1.0 (1)
20a	1.06	2.65 (0.4)	3.16 (0.3)	0.8	1.3 (0.6)
20b	>6.40	>6.40	>6.40	>25	nd

[a] Thermally adapted state (dark) compared to the PSS following 365 nm irradiation. The MIC was determined on *E. coli* BW25113 by fitting a Gompertz equation to the growth inhibition curve, and the in vitro activity was determined with an *E. coli* gyrase supercoiling assay. Numbers in brackets display the fold-difference in activity between dark vs. irradiated states. nd = not determined.

azo and hydrazone functional groups. The comparison of the UV spectra of mono photoswitches **6a** and **10a** and the double switch **19a** after irradiation with 365 nm light revealed a clear difference. For both compounds incorporating a single photoswitch, irradiation led to a constant or lowered absorption maximum at around 300 nm, while for the double photoswitch, an increase was observed (Figure 4A, Figure 2B and Supporting Information Figures S5, S6 and S8). A similar trend can be observed comparing the absorption maxima at 350 nm for the monoswitch **10c** with the doubleswitch **20a**. At higher wavelengths two distinct maxima at 408 and 430 nm strongly increased after irradiation in **20a**, as observed for **10c**. A precise determination of the four isomeric states at the PSS was not possible by chromatographic analysis (LC/UV/MS). This was because the presence of only two peaks could be detected after irradiation, presumably due to coelution of the *C*-terminal photoisomers. Based on the chromatographic behavior of the monoswitches (see above), we assume that the two peaks correspond to *N*-terminal isomers, and based on this determined the *N*-terminal *cis* fraction to be about 60% for double photoswitches **19a** and **20a**. Four switching cycles with alternating light of 365 and 450 nm showed that **20a** was fatigue-resistant, whereas **19a** lost absorbance intensity over the switching cycles, suggesting degradation (Figure 4B and Supporting Information Figure S9). According to kinetic experiments, the half-lives for the thermal relaxation to the ground state at 35 °C for these two molecules were 14.9 h for **19a** and 6.9 h for **20a**.

The effect of the photoisomerization on the antimicrobial properties was assessed as described above with pre-irradiation of a solution of the antibiotic, followed by bacterial incubation and eventually read out of MICs. Because the compounds had additional absorbance bands at higher wavelengths, they were also excited at 450 nm to induce a photoisomerization. Interestingly, irradiation of **20a** with this wavelength entailed a significant increase of the absorption maximum at 350 nm and a decrease of the absorption band between 400 and 450 nm (Figure 4A). Samples of **20a** exposed to light showed an increase of the MIC from 1.06 to 2.65 µg/mL. The data were corroborated by the enzymatic assay, where irradiation of **20a** led to a 1.6 fold decrease in gyrase inhibition, indicating that isomerization of both sides of the molecule at the same time is deleterious for the antimicrobial activity. Thus, while light irradiation led to an increase of antibacterial potency in *N*-terminally modified cystobactamids and a decrease in *C*-terminally modified compounds, the latter effect was prevalent in the combination of the two motifs.

Addressing resistance mechanisms with light

The possibility to influence bacterial resistance with light is one of the major advantages offered by photoswitchable antibiotics, nevertheless clear proof-of-principles are missing. We therefore exposed the photoswitchable cystobactamids to two of the known resistance mechanisms for the structurally related

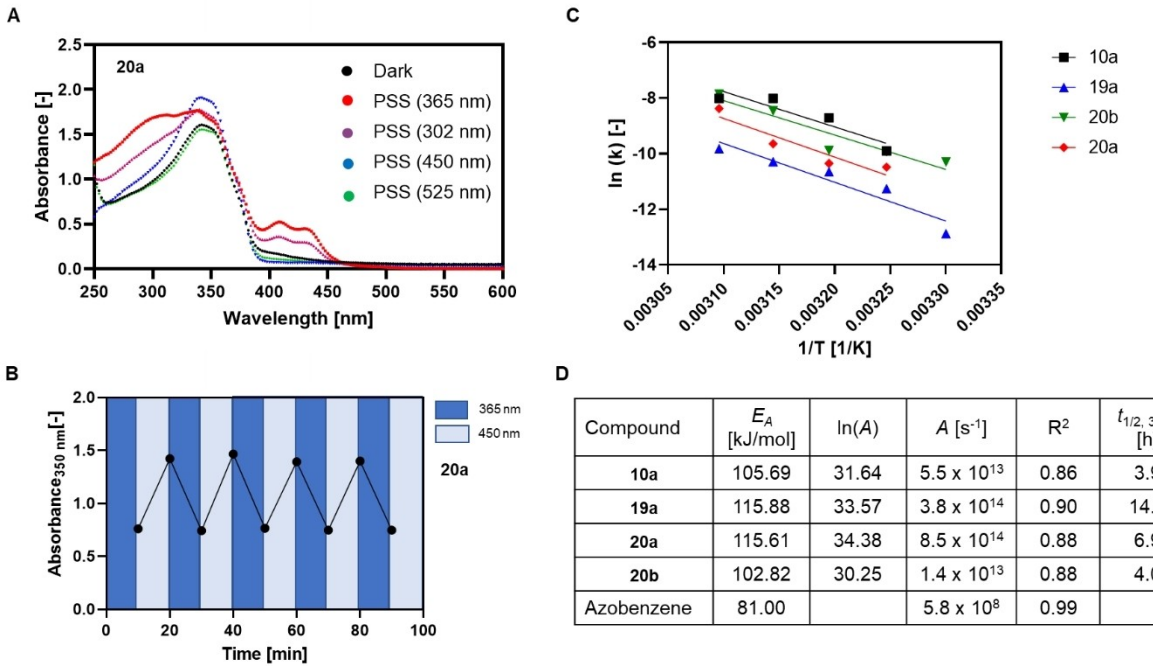

Compound	E_A [kJ/mol]	ln(*A*)	*A* [s^{-1}]	R^2	$t_{1/2,\ 35°C}$ [h]
10a	105.69	31.64	5.5×10^{13}	0.86	3.9
19a	115.88	33.57	3.8×10^{14}	0.90	14.9
20a	115.61	34.38	8.5×10^{14}	0.88	6.9
20b	102.82	30.25	1.4×10^{13}	0.88	4.0
Azobenzene	81.00		5.8×10^{8}	0.99	

Figure 4. Characterization of doubly switchable cystobactamids. A) UV spectra of **20a** (0.5 mM in DMSO) in its thermally adapted state before irradiation (in black) and after irradiation with light of five different wavelengths; B) Repeated photoswitching of **20a**, recorded by the UV absorption at 350 nm after alternating irradiation with 365 nm light (dark blue periods) and 450 nm (light blue periods). C) Arrhenius plot of the logarithmic rate constants of thermal isomerization to the ground state versus reciprocal temperature for four cystobactamids. D) Kinetic data for **10a**, **19a**, **20b** and **20a**. Activation energy E_A and half-life $t_{1/2}$ were calculated based on reaction speeds in a temperature range from 30–50 °C (Supporting Information Figures S10–S21, Table S3). Data for azobenzene were taken from Ref. [21].

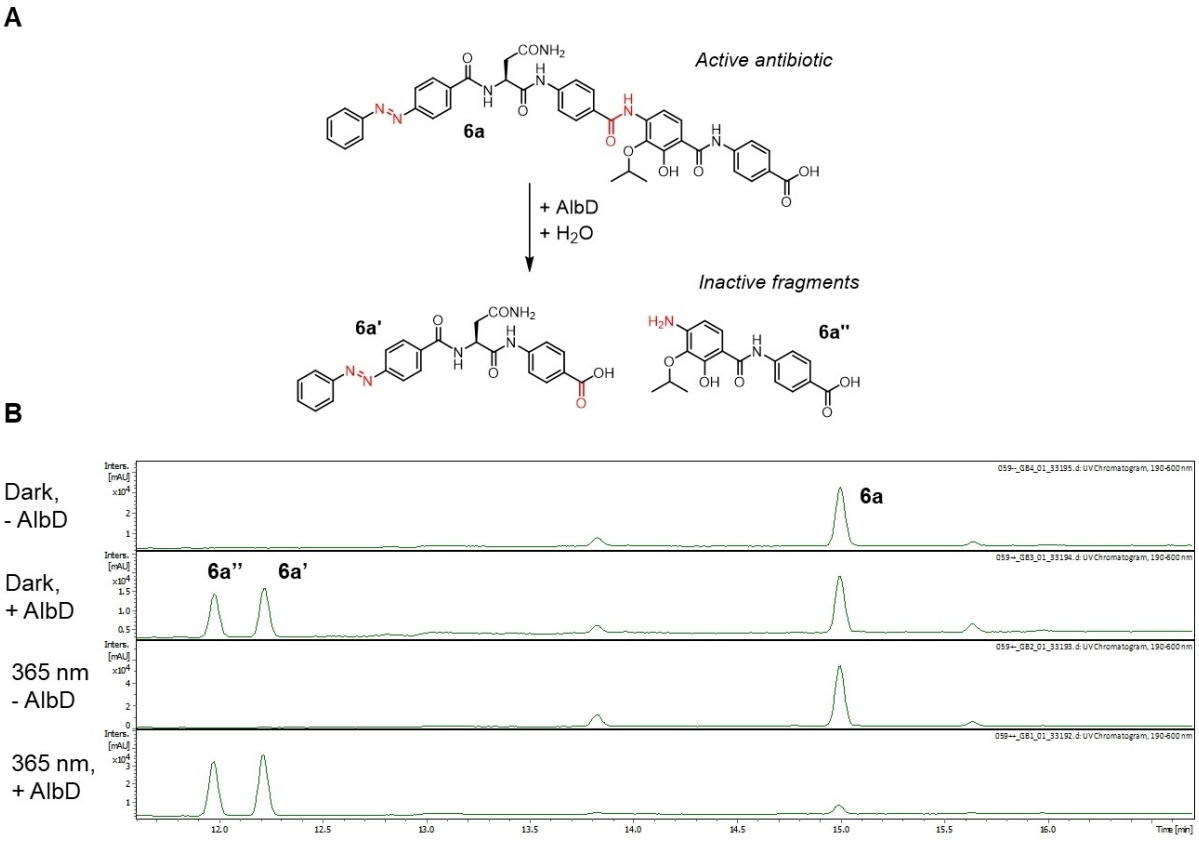

Figure 5. Light-dependent inactivation of photoswitchable cystobactamids by AlbD. A) Enzymatic reaction. The photoswitchable moiety and the cleavage site are marked in red. B) LC/UV-chromatographic traces of **6a** after 30 minutes incubation, in presence (+) or absence (−) of AlbD. Before incubation, **6a** was either irradiated (365 nm) or not (dark).

albicidin, the endopeptidase AlbD and the high affinity binding protein AlbA.[10e,g]

For the former we made use of a biochemical assay that monitors the proteolytic activity of recombinant AlbD in vitro using LC/UV/MS.[10e] Albicidin was completely cleaved within 30 minutes, and similar results were obtained for the cystobactamid **2**. We wondered whether photoswitchable cystobactamids were also recognized by AlbD, and whether their cleavage rates differed between the isomeric states. Both types of monoswitchable as well as a doubly photoswitchable cystobactamid were substrates of the endopeptidase (Figure 5 and Supporting Information Figure S22), but **10a** and **19a** were degraded to a larger extent after 30 min than **6a**, with 40% of the compound remaining. Interestingly, shining 365 nm light on **6a** considerably accelerated the cleavage, with only 7% of the antibiotic remaining after the same time (Table 3). This suggests that a *cis*-configured **6a** is a better substrate for the endopeptidase than its *trans*-isomer.

In order to probe the impact of the resistance factor AlbA, we assessed the antibiotic properties of selected photoswitchable cystobactamids against *E. coli* in presence of AlbA in an agar diffusion assay.[10g] Three photoswitchable cystobactamids (one representative per subgroup) and the nonswitchable controls albicidin and **3** were tested. The antibiotic activity of albicidin disappeared in the presence of AlbA, while the cystobactamid **3** was not affected (Figure 6 and Table 4); the findings are consistent with previous reports.[10f,g] Also the *C*-terminally modified **10a** escaped the binding protein. In contrast, the activity of **19a** was neutralized by the presence of AlbA, no matter whether the sample was pre-irradiated or not. Most interesting was the azobactamid **6a**, differing from **3** by the azo group instead of the amide connecting rings A and B. Its inhibition of microbial growth was not impaired by AlbA in the dark, but upon irradiation, the antibiotic activity was completely lost. This is remarkable, given that the generated *cis*-isomer has higher antimicrobial activity in the absence of AlbA (Table 1). The finding implies that the two photoisomeric states of **6a** have significantly different affinities for the

Table 3. Light-dependent inactivation of photoswitchable cystobactamids by AlbD.[a]

Compound	% non-cleaved in presence of AlbD	
	Dark	365 nm
Albicidin	0	nd
6a	40	7
10a	21	23
19a	14	9

[a] Residual percentage of intact antibiotic with and w/o irradiation after 30 min incubation with AlbD.

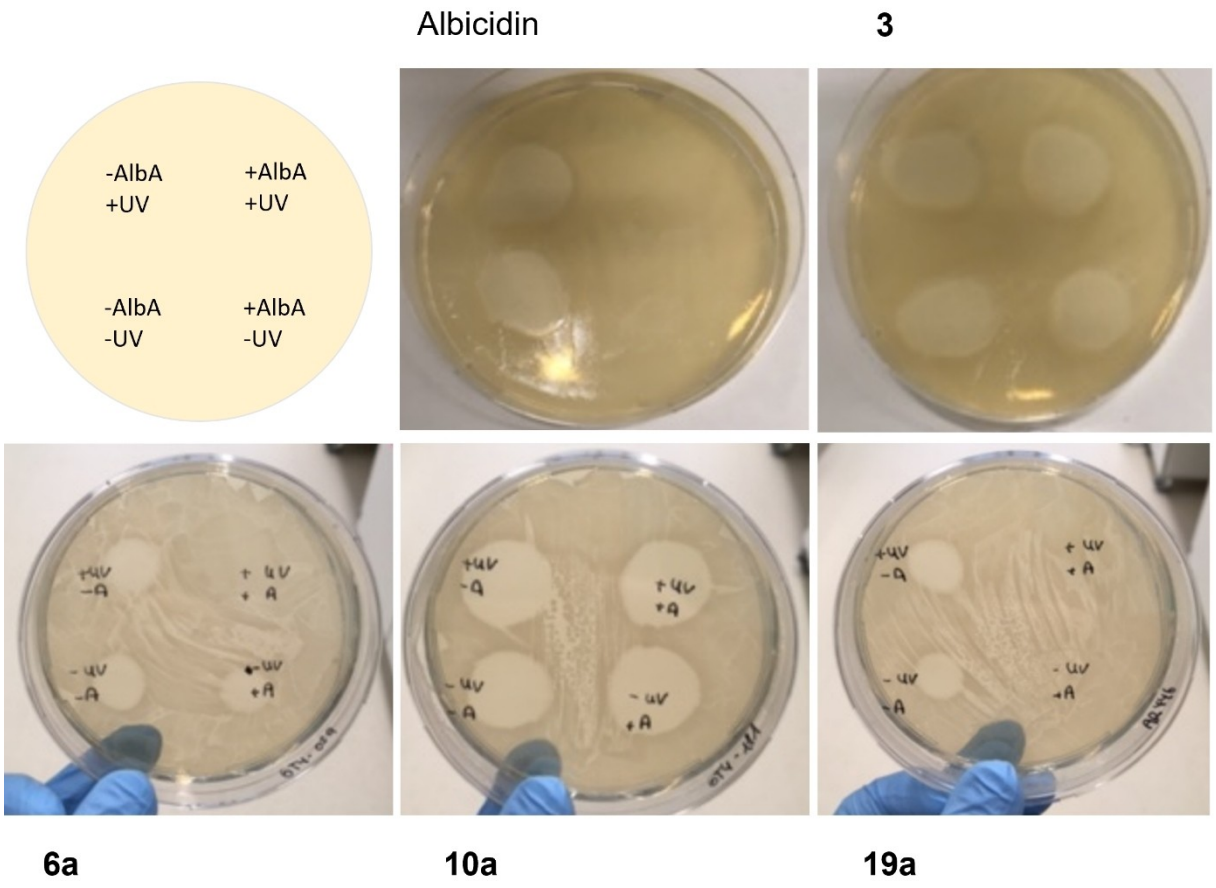

Figure 6. Light-dependent inactivation of photoswitchable cystobactamids by AlbA. Top left: Petri plate layout. Other panels: Images of the Petri plates from the agar diffusion assay. Albicidin or cystobactamids were pre-irradiated with 365 nm light (+ UV) or not (-UV), deposited on an agar plate inoculated with *E. coli* BW25113 in the presence (+) or absence (−) of AlbA (1 equivalent). Growth inhibition was visible as an inhibition zone, whose diameter was measured and listed in Table 4.

Table 4. Light-dependent inactivation of photoswitchable cystobactamids by AlbA.[a]

	Inhibition zone [cm]			
	+AlbA		-AlbA	
	Dark	365 nm	Dark	365 nm
Albicidin	0	0	2.2	2.2
3	2.1	2.1	2.5	2.5
6a	1.3	0	1.3	1.3
10a	2.2	2.2	2.2	2.2
19a	0	0	1.4	1.4

[a] Results summary of agar diffusion assays in *E. coli* BW25113 as depicted in Figure 6.

resistance protein, and the *cis*-isomer is recognized as substrate, while the *trans*-isomer is not or has a considerably lower binding affinity. Taken together, the experiments showed a steep SAR behind the antibiotic-AlbA interaction and notably, revealed that a bacterial resistance mechanism could be modulated by light.

Discussion

Photopharmacology has been proposed as an innovative approach to tackle the problem of bacterial resistance, because it offers the possibility to selectively control antibiotic activity with light. Since the first report of a photoswitchable antibacterial agent in 2013, significant progress has been made towards the creation of the ideal photoantibiotic that should possess large differences (ON/OFF) in activity between two isomers and be quantitatively switched with visible light to ensure optimal tissue penetration, while minimizing radiation damaging.[2g,6, 16c] This is exemplified by an azo-trimethoprim analog that was activated with red light to give two isomeric states with an eight-fold difference in potency.[7a]

This work widens photoswitchable drug design in several aspects. One concerns the successful application of acylhydrazones in photopharmacology. Acylhydrazones have favorable photochemical properties[2d] and avoid a metabolic liability compared to azobenzenes, because the reduction of the latter in vivo may generate free and potentially toxic anilines, as exemplified by Prontosil Rubrum.[22] On the other hand, also acylhydrazones have stability issues, as they might hydrolyse into an aldehyde and a hydrazide under acidic pH, and have

therefore been red-flagged.[23] However, acylhydrazone-containing drugs have progressed to clinical development,[24] and further applications in photopharmacology deserve being explored.

We also report compounds with a dual photoswitch; in principle, such molecules can adopt four light-dependent states, i.e. A–B, A′–B, A–B′ and A′–B′.[21] We found that cystobactamids with dual photoswitches indeed possess unique properties compared to the monoswitches. However, the current compounds face limitations, as individual regioisomers cannot be independently, selectively switched by light; thus, their structural composition could not be properly defined.

The proof-of-concept that photoswitchable antibiotics are principally feasible has been built on established antibiotics like ciprofloxacin, trimethoprim or gramicidin. However, the need for novel chemical scaffolds to build a next generation of antibiotics, rather than further modifying existing classes, has been clearly articulated.[25] We addressed this need by selecting a novel and promising class of natural products, the cystobactamids, as the basis for photoswitchable antibiotics. We identified both *N*- and *C*- termini of the scaffold as suitable sites for the insertion of photoswitches, replacing the original amide bonds that connect the aromatic units. The modifications were in general well tolerated, as the potent antimicrobial properties against *E. coli* were retained. In sum, twenty photoresponsive cystobactamids were synthesized that were categorized in three subgroups, i.e. mono *N*-terminal, mono *C*-terminal and doubly photoswitchable cystobactamids. While irradiation led to an increase in antibiotic activity for compounds incorporating an *N*-terminal photoswitch, the opposite was found for *C*-terminal modifications. The antimicrobial activities observed in the cellular assay were corroborated by a biochemical assay measuring gyrase inhibition. This indicated that photo-induced isomerization leads to different abilities to interact with the enzymatic target. However, differences in antimicrobial properties were moderate overall.

The current concept of a photoswitchable antibiotic foresees a light-induced activation of the drug, meaning that the molecule is stored in its inactive form, and the active species is generated upon irradiation with light in situ, and disappears over time by thermal relaxation. In this study instead, light-induced inactivation was observed for some compounds like **19a**, enabling a reverse approach. The compound is taken in the thermally adapted form as an active substance, exerting its function in the body without the needs of reliable activation by light as well as assuring pharmacokinetics and -dynamics of two isomers. This would be particularly relevant for infections at deep, poorly accessible body sites that require sustained exposure at high concentrations; it also avoids resistance formation under selection pressure conditions, that would be induced by isomerization to a less active isomer. In contrast, 'reverse' order compounds as found here can be inactivated by light 'on demand'; natural light could convert and keep the antibiotic in the inactive state. However, their application is hampered by the incomplete conversion to the *cis* form as well as its transient nature. Also the often limited exposure to light in the environment constitutes a limitation for such agents.

We also investigated whether two classical resistance mechanisms, antibiotic degradation and antibiotic trapping, can be modulated by light. For the endopeptidase AlbD, we observed that conformational changes near the *N*-terminus influenced the rate of proteolysis of the antibiotic **6a**. This implies that structural variations in this region, although far from the cleavage site, can alter the function of the resistance factor. In addition, we investigated whether the neutralization of cystobactamids by the binding protein AlbA was affected by isomerization. We observed that the thermal *trans*-isomer was not trapped by AlbA, whereas the *cis*-isomer was. The high importance of the A–B rings for the antibacterial activity has been described before; the current findings underline that also the sensitivity towards resistance factors can be tuned by this region of the molecule.

Conclusions

The study provides evidence that light-induced conformational changes alter the resistance properties of the compounds and expands the arsenal of photoswitchable antibiotics based on the unusual cystobactamid scaffold. Their oligoaryl nature renders cystobactamids well-suited to incorporating photoswitches and optimizing them towards improved on–off activities seems an attractive target of future studies.

Methods

Chemical synthesis

See Supporting Information

Irradiation of compounds

The photoswitchable cystobactamids were irradiated by LEDs with defined wavelengths (Sahlmann Photochemical Solutions, type: 3x Nichia NCSU276 A). Available wavelengths were 340 nm, 365 nm, 450 nm, 495 nm, 525 nm and 617 nm. The compounds were dissolved in DMSO at a concentration of 0.5 mM and irradiated at an intensity of 780 mW for 1 h unless indicated otherwise. The cystobactamids were transferred to a microtiter plate and placed in a polystyrene box. The lid of the box had a hole to fit the LED and to ensure the same distance of approx. 15 cm between LED and sample for all experiments.

Determination of the photo-stationary state (PSS) by LC/MS

The photo-stationary state was determined by LC/UV/MS measurements using the same method as described for the AlbD assay. The samples were measured in positive mode over a mass range of 50–1500 m/z. By integration of the UV chromatographic peak areas corresponding to the *cis* and *trans* isomers, the ratio between *cis* and *trans* was calculated.

Determination of minimal inhibitory concentrations (MICs)

The MIC was determined on *Escherichia coli* BW25113. For the preparation of bacteria, an overnight culture was inoculated in Mueller-Hinton broth and incubated for approximately 18 h at 37 °C, 150 rpm. The overnight culture was diluted in fresh media to $OD_{600} = 0.1$ and grown to $OD_{600} = 0.5$ before being diluted to $OD_{600} = 0.01$. From a stock solution of the respective compound in DMSO (0.5 mg/ml) – either in ground state or irradiated for 1 h at 365 nm – a three-fold dilution series was prepared. For the treatment, 1.92 µl of each dilution were transferred to a 96 well plate and mixed with 148 µl of the bacterial culture resulting in compound concentrations in the range of 6.4 to 0.0001 µg/ml. The plate was sealed and incubated for 18 h at 37 °C. The optical density after 18 h was determined using a microplate reader (Biomek, Powerwave XS). The OD_{600}-values were then plotted against the log(concentration) of the compound and fitted with a Gompertz-equation in GraphPad Prism to determine the MIC values.

DNA negative supercoiling assay, determination of IC_{50} values

The concentration at which 50% of gyrase activity inhibition occurs (IC_{50}) was determined by using commercial *E. coli* DNA gyrase (Inspiralis, UK) and pUC19 relaxed DNA. The gyrase mix was prepared according to the supplier manual and 11 µl were transferred to 0.2 ml Eppendorf cups. The compound at a stock concentration of 0.75 µM in DMSO – either in ground state or irradiated for 1 h at 365 nm – was pre-diluted to 0.375 µM in water. The pre-diluted compound was used to prepare a three-fold dilution series down to 0.03 µM, of which 1 µl was transferred to the gyrase mix. After a mixing step and spinning down, 25 ng relaxed pUC19 DNA was added and the final solution (volume: 15 µl) was incubated for 30 min at 37 °C. The enzymatic reaction was stopped by increasing the temperature to 60 °C for 10 min. After addition of 3 µl DNA loading dye, the samples were loaded on a 0.8% agarose gel and run for 30 min at 100 V. The gel was stained in a 0.1 µg/ml ethidium bromide solution and scanned (ChemiDoc, Biorad). Since gyrase supercoils the DNA, the band intensity for supercoiled DNA was used to determine the inhibitory effect of the compound – with a non-treated control as reference. For an active compound, the intensity of the supercoiled form decreases with increasing concentration of the compound. The intensities were then plotted against the log(concentration) of the compound and the IC_{50} values was determined using a non-linear log(inhibitor) versus response fit in GraphPad Prism.

AlbD Assay

Pure AlbD protein was obtained by recombinant expression and the AlbD assay was performed according to our previous work[11] with the ground state cystobactamid, the switched version and albicidin as positive control. 24 µM of AlbD were incubated with 12 µM of compound in 0.2 M phosphate buffer for 30 min at 28 °C. In parallel for each compound, a sample without enzyme was generated to prove compound stability over incubation time. 350 µl methanol were added to precipitate the protein. The precipitate was separated by 20 min centrifugation at 20,000g. 250 µl of the supernatant were transferred to a fresh vial and evaporated in a speed vac (Eppendorf, Concentrator plus). The dried concentrate was resupended in 100 µl methanol and analyzed via LC/MS measurement. 3 µl per sample were injected into an Ultra high pressure chromatography instrument (UHPLC) (Thermo, Dionex Ultimate 3000) with a C18 column (Phenomenex, Kinetex 1.7 µm C18 150×2.1 mm). A 30 min linear gradient with 99% A and 1% B to 100% B was used to separate the sample components – with A water + 0.1% formic acid and B acetonitrile + 0.1% formic acid. The masses were detected with a quadrupole time of flight mass spectrometer (maXis HD QTof, Bruker Daltonics, Bremen, Germany) after electrospray ionization. The measurement was performed in positive ion mode in a mass range from 50–1500 m/z. The resulting data was analyzed using DataAnalysis (Bruker Daltonics, Bremen, Germany).

AlbA Assay

Pure AlbA protein was obtained as reported under Ref. [10g]. The AlbA assay was performed according to Rostock et al.[10f] The compounds (0.5 mg/ml in DMSO) were either stored in the dark or irradiated at 365 nm for 1 h. Albicidin was used in parallel to prove resistance protein activity. Afterwards 1.5 µl of the compound or DMSO as negative control were added to 4.2 µl AlbA (4.5 mg/ml) or PBS as enzyme-free control. PBS was added to reach a total volume of 15 µl. The samples were incubated for 20 min at room temperature in the dark to allow the binding event to take place. In the meantime, 100 µl of an *E. coli* BW25113 culture grown in LB-broth to $OD_{600} = 0.5$ was equally spread on a LB-agar plate. The 15 µl compound-protein mix was added as a dot on the agar plate and after letting it dry, incubated for 18 h at 37 °C. The diameter of the inhibition area was measured.

Authors contribution

GT and MB designed the study; GT, JR, AR, HP and JK performed and enabled the experiments; GT, JR and MB analyzed the data; GT, JR, and MB wrote the manuscript.

Funding

The study received funding from the Bundesministerium für Bildung und Forschung (BMBF, Opcybac 16GW0219K), the German Center for Infection Research (DZIF, TTU09.722), and the Helmholtz Association (VH-GS-202).

Acknowledgements

The authors are thankful to Ulrike Beutling and Heike Overwin for HRMS and LCMS measurements, Frank Surup and Christel Kakoschke for NMR measurements, and Tim Mollner for

building block supply. Open Access funding enabled and organized by Projekt DEAL.

Conflict of Interest

GT, MB, and AR are coinventors on a patent application on synthetic cystobactamids.

Data Availability Statement

The data that support the findings of this study are available in the supplementary material of this article.

Keywords: antibiotics · antimicrobial resistance · natural products · oligoarylamides · photopharmacology

[1] a) J. Broichhagen, J. A. Frank, D. Trauner, *Acc. Chem. Res.* **2015**, *48*, 1947–1960; b) M. M. Lerch, M. J. Hansen, G. M. van Dam, W. Szymanski, B. L. Feringa, *Angew. Chem. Int. Ed. Engl.* **2016**, *55*, 10978–10999; c) W. A. Velema, W. Szymanski, B. L. Feringa, *J. Am. Chem. Soc.* **2014**, *136*, 2178–2191; d) K. Hüll, J. Morstein, D. Trauner, *Chem. Rev.* **2018**, *118*, 10710–10747.

[2] a) A. A. Beharry, G. A. Woolley, *Chem. Soc. Rev.* **2011**, *40*, 4422–4437; b) C. Brieke, F. Rohrbach, A. Gottschalk, G. Mayer, A. Heckel, *Angew. Chem. Int. Ed. Engl.* **2012**, *51*, 8446–8476; c) R. Klajn, *Chem. Soc. Rev.* **2014**, *43*, 148–184; d) D. J. van Dijken, P. Kovaricek, S. P. Ihrig, S. Hecht, *J. Am. Chem. Soc.* **2015**, *137*, 14982–14991; e) M. W. H. Hoorens, M. Medved, A. D. Laurent, M. Di Donato, S. Fanetti, L. Slappendel, M. Hilbers, B. L. Feringa, W. Jan Buma, W. Szymanski, *Nat. Commun.* **2019**, *10*, 2390; f) M. Medved, M. W. H. Hoorens, M. Di Donato, A. D. Laurent, J. Fan, M. Taddei, M. Hilbers, B. L. Feringa, W. J. Buma, W. Szymanski, *Chem. Sci.* **2021**, *12*, 4588–4598; g) O. Babii, S. Afonin, M. Berditsch, S. Reibetaer, P. K. Mykhailiuk, V. S. Kubyshkin, T. Steinbrecher, A. S. Ulrich, I. V. Komarov, *Angew. Chem. Int. Ed. Engl.* **2014**, *53*, 3392–3395; h) H. B. Cheng, S. Zhang, E. Bai, X. Cao, J. Wang, J. Qi, J. Liu, J. Zhao, L. Zhang, J. Yoon, *Adv. Mater.* **2021**, e2108289.

[3] a) E. Tacconelli, E. Carrara, A. Savoldi, S. Harbarth, M. Mendelson, D. L. Monnet, C. Pulcini, G. Kahlmeter, J. Kluytmans, Y. Carmeli, M. Ouellette, K. Outterson, J. Patel, M. Cavaleri, E. M. Cox, C. R. Houchens, M. L. Grayson, P. Hansen, N. Singh, U. Theuretzbacher, N. Magrini, *Lancet Infect. Dis.* **2018**, *18*, 318–327; b) C. Årdal, M. Balasegaram, R. Laxminarayan, D. McAdams, K. Outterson, J. H. Rex, N. Sumpradit, *Nat. Rev. Microbiol.* **2020**, *18*, 267–274.

[4] a) M. C. Schneider, C. Munoz-Zanzi, K.-d. Min, S. Aldighieri, *"One Health" From Concept to Application in the Global World*, Oxford University Press, **2019**; b) J. S. Mackenzie, M. Jeggo, *Trop. Med. Infect. Dis.* **2019**, *4*.

[5] a) M. Lakemeyer, W. Zhao, F. A. Mandl, P. Hammann, S. A. Sieber, *Angew. Chem. Int. Ed. Engl.* **2018**, *57*, 14440–14475; b) U. Theuretzbacher, L. J. V. Piddock, *Cell Host Microbe* **2019**, *26*, 61–72; c) K. Lewis, *Cell* **2020**, *181*, 29–45.

[6] W. A. Velema, J. P. van der Berg, M. J. Hansen, W. Szymanski, A. J. Driessen, B. L. Feringa, *Nat. Chem.* **2013**, *5*, 924–928.

[7] a) M. Wegener, M. J. Hansen, A. J. M. Driessen, W. Szymanski, B. L. Feringa, *J. Am. Chem. Soc.* **2017**, *139*, 17979–17986; b) W. A. Velema, M. J. Hansen, M. M. Lerch, A. J. Driessen, W. Szymanski, B. L. Feringa, *Bioconjugate Chem.* **2015**, *26*, 2592–2597; c) Z. Li, Y. Wang, M. Li, H. Zhang, H. Guo, H. Ya, J. Yin, *Org. Biomol. Chem.* **2018**, *16*, 6988–6997; d) E. Contreras-García, D. Martínez-López, C. A. Alonso, C. Lozano, C. Torres, M. A. Rodríguez, P. J. Campos, D. Sampedro, *Eur. J. Org. Chem.* **2017**, *2017*, 4719–4725; e) Y. Q. Yeoh, J. Yu, S. W. Polyak, J. R. Horsley, A. D. Abell, *ChemBioChem* **2018**, *19*, 2591–2597; f) X. Just-Baringo, A. Yeste-Vázquez, J. Moreno-Morales, C. Balleste-Delpierre, J. Vila, E. Giralt, *Chem. Eur. J.* **2021**, *27*, 12987–12991; g) O. Babii, S. Afonin, A. Y. Ishchenko, T. Schober, A. O. Negelia, G. M. Tolstanova, L. V. Garmanchuk, L. I. Ostapchenko, I. V. Komarov, A. S. Ulrich, *J. Med. Chem.* **2018**, *61*, 10793–10813.

[8] A. I. Lauxen, P. Kobauri, M. Wegener, M. J. Hansen, N. S. Galenkamp, G. Maglia, W. Szymanski, B. L. Feringa, O. P. Kuipers, *Pharmaceuticals (Basel)* **2021**, *14*.

[9] a) S. M. Hashimi, M. K. Wall, A. B. Smith, A. Maxwell, R. G. Birch, *Antimicrob. Agents Chemother.* **2007**, *51*, 181–187; b) S. Baumann, J. Herrmann, R. Raju, H. Steinmetz, K. I. Mohr, S. Huttel, K. Harmrolfs, M. Stadler, R. Muller, *Angew. Chem. Int. Ed.* **2014**, *53*, 14605–14609; c) S. Cociancich, A. Pesic, D. Petras, S. Uhlmann, J. Kretz, V. Schubert, L. Vieweg, S. Duplan, M. Marguerettaz, J. Noell, I. Pieretti, M. Hugelland, S. Kemper, A. Mainz, P. Rott, M. Royer, R. D. Sussmuth, *Nat. Chem. Biol.* **2015**, *11*, 195–197; d) S. M. Hashimi, *J. Antibiot.* **2019**, *72*, 785–792; e) S. Huttel, G. Testolin, J. Herrmann, T. Planke, F. Gille, M. Moreno, M. Stadler, M. Bronstrup, A. Kirschning, R. Muller, *Angew. Chem. Int. Ed.* **2017**, *56*, 12760–12764.

[10] a) M. J. Walker, R. G. Birch, J. M. Pemberton, *Mol. Microbiol.* **1988**, *2*, 443–454; b) W. V. Basnayake, R. G. Birch, *Microbiology* **1995**, *141 (Pt 3)*, 551–560; c) L. Zhang, R. G. Birch, *Proc. Natl. Acad. Sci. USA* **1997**, *94*, 9984–9989; d) L. Zhang, J. Xu, R. G. Birch, *Microbiology* **1998**, *144 (Pt 2)*, 555–559; e) L. Vieweg, J. Kretz, A. Pesic, D. Kerwat, S. Gratz, M. Royer, S. Cociancich, A. Mainz, R. D. Sussmuth, *J. Am. Chem. Soc.* **2015**, *137*, 7608–7611; f) L. Rostock, R. Driller, S. Gratz, D. Kerwat, L. von Eckardstein, D. Petras, M. Kunert, C. Alings, F. J. Schmitt, T. Friedrich, M. C. Wahl, B. Loll, A. Mainz, R. D. Sussmuth, *Nat. Commun.* **2018**, *9*, 3095; g) A. Sikandar, K. Cirnski, G. Testolin, C. Volz, M. Bronstrup, O. V. Kalinina, R. Muller, J. Koehnke, *J. Am. Chem. Soc.* **2018**, *140*, 16641–16649.

[11] G. Testolin, K. Cirnski, K. Rox, H. Prochnow, V. Fetz, C. Grandclaudon, T. Mollner, A. Baiyoumy, A. Ritter, C. Leitner, J. Krull, J. van den Heuvel, A. Vassort, S. Sordello, M. M. Hamed, W. A. M. Elgaher, J. Herrmann, R. W. Hartmann, R. Müller, M. Brönstrup, *Chem. Sci.* **2020**, *11*, 1316–1334.

[12] a) M. Moeller, M. D. Norris, T. Planke, K. Cirnski, J. Herrmann, R. Müller, A. Kirschning, *Org. Lett.* **2019**, *21*, 8369–8372; b) T. Planke, K. Cirnski, J. Herrmann, R. Muller, A. Kirschning, *Chemistry* **2020**, *26*, 4289–4296; c) I. Behroz, L. Kleebauer, K. Hommernick, M. Seidel, S. Gratz, A. Mainz, J. B. Weston, R. Sussmuth, *Chemistry* **2021**; d) L. Zborovsky, L. Kleebauer, M. Seidel, A. Kostenko, L. von Eckardstein, F. O. Gombert, J. Weston, R. D. Süssmuth, *Chem. Sci.* **2021**, *12*, 14606–14617.

[13] M. Schoenberger, A. Damijonaitis, Z. Zhang, D. Nagel, D. Trauner, *ACS Chem. Neurosci.* **2014**, *5*, 514–518.

[14] B. F. Lui, N. T. Tierce, F. Tong, M. M. Sroda, H. Lu, J. Read de Alaniz, C. J. Bardeen, *Photochem. Photobiol. Sci.* **2019**, *18*, 1587–1595.

[15] W. A. M. Elgaher, M. M. Hamed, S. Baumann, J. Herrmann, L. Siebenbürger, J. Krull, K. Cirnski, A. Kirschning, M. Brönstrup, R. Müller, R. W. Hartmann, *Chemistry* **2020**, *26*, 7219–7225.

[16] a) C. Knie, M. Utecht, F. Zhao, H. Kulla, S. Kovalenko, A. M. Brouwer, P. Saalfrank, S. Hecht, D. Bleger, *Chemistry* **2014**, *20*, 16492–16501; b) D. Bleger, S. Hecht, *Angew. Chem. Int. Ed. Engl.* **2015**, *54*, 11338–11349; c) M. Dong, A. Babalhavaeji, S. Samanta, A. A. Beharry, G. A. Woolley, *Acc. Chem. Res.* **2015**, *48*, 2662–2670; d) D. Bleger, J. Schwarz, A. M. Brouwer, S. Hecht, *J. Am. Chem. Soc.* **2012**, *134*, 20597–20600.

[17] C. E. Weston, R. D. Richardson, P. R. Haycock, A. J. White, M. J. Fuchter, *J. Am. Chem. Soc.* **2014**, *136*, 11878–11881.

[18] M. Lepeltier, O. Lukoyanova, A. Jacobson, S. Jeeva, D. F. Perepichka, *Chem. Commun.* **2010**, *46*, 7007–7009.

[19] M. M. Lerch, M. J. Hansen, W. A. Velema, W. Szymanski, B. L. Feringa, *Nat. Commun.* **2016**, *7*, 12054.

[20] M. J. Hansen, M. M. Lerch, W. Szymanski, B. L. Feringa, *Angew. Chem. Int. Ed. Engl.* **2016**, *55*, 13514–13518.

[21] F. Zhao, L. Grubert, S. Hecht, D. Bléger, *Chem. Commun.* **2017**, *53*, 3323–3326.

[22] W. G. Levine, *Drug Metab. Rev.* **1991**, *23*, 253–309.

[23] J. B. Baell, L. Ferrins, H. Falk, G. Nikolakopoulos, *Aust. J. Chem.* **2013**, *66*, 1483–1494.

[24] H. S. Roth, P. J. Hergenrother, *Curr. Med. Chem.* **2016**, *23*, 201–241.

[25] U. Theuretzbacher, S. Gottwalt, P. Beyer, M. Butler, L. Czaplewski, C. Lienhardt, L. Moja, M. Paul, S. Paulin, J. H. Rex, L. L. Silver, M. Spigelman, G. E. Thwaites, J.-P. Paccaud, S. Harbarth, *Lancet Inf. Dis.* **2019**, *19*, e40-e50.

Manuscript received: April 26, 2022
Accepted manuscript online: June 30, 2022
Version of record online: August 3, 2022